

# SATURATION EFFECT ON VUV COHERENT HARMONIC GENERATION AT UVSOR-II

T. Tanikawa<sup>\*,#</sup>, M. Adachi, M. Katoh, J. Yamazaki, H. Zen,  
 UVSOR Facility, Institute for Molecular Science, Okazaki, 4448585, Japan  
 Y. Taira, M. Hosaka, N. Yamamoto,  
 Nagoya University, Nagoya, 4648603, Japan

## Abstract

Synchrotron radiation source to generate a coherent light by using a laser seeding technique are under development at the UVSOR-II. In the past experiments, we have succeeded in generating coherent harmonics (CHs) in deep ultraviolet (DUV) and vacuum ultraviolet (VUV) region and also in generating CHs with variable polarizations in DUV region.

This time we have successfully observed CHs up to the 9<sup>th</sup> harmonic over a wide peak power range regime, for the first time. In addition, we observed CH intensity oscillations after the first maximum. In this paper, we discuss the results of some systematic measurements and those analytical and particle tracking simulations.

## INTRODUCTION

The laser seeding technique, injecting laser with full coherence to electron bunch into undulator, is used for single-pass seeded free-electron laser (FEL) [1] to improve temporal coherence of self-amplified spontaneous emission (SASE)-FEL, for coherent harmonic generation (CHG) [2-4], and for high-gain harmonic generation (HG) [5].

At UVSOR-II, a 750 MeV synchrotron light source, a resonator-type FEL has been studied for many years [6-8]. These years, by utilizing a part of the FEL system, studies on coherent synchrotron radiation (CSR) in terahertz range and CHG in DUV range have been performed by using a femto-second laser system. In the past studies, DUV CHs with circular polarization have been successfully generated [9-10]. In addition, the CHG in VUV region has successfully been measured up to 9<sup>th</sup> harmonic.

## EXPERIMENTAL SETUP

### Configuration

Figure 1 illustrates the experimental setup. Femto-second Ti: Sapphire laser system for injection laser consist of a mode-locked oscillator (Mira, COHERENT), which is synchronized with the RF acceleration of the storage ring, and a regenerative amplifier (Legend, COHERENT). The laser pulse is injected with 1 kHz repetition rate via a sapphire window. A wave plate and polarizer for changing laser power, a lens pair for beam expander, and a focusing lens (5000 mm of focal length) are settled upstream of the sapphire window and the laser

pulse is focused into the modulator part of optical klystron (OK). The CHs generated by the interaction between the laser pulse and the electron beam are introduced to a light diagnostics section or to a VUV spectrometer.

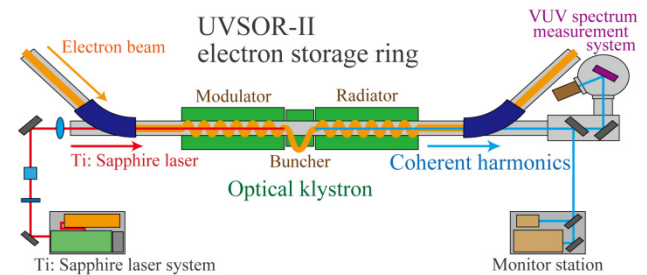


Figure 1: Schematic drawing of experimental setup in coherent harmonic generation experiment.

### Parameters

Table 1 shows parameters of the electron beam, the OK, and Ti: Sapphire laser in this experiment.

Table 1: Experimental Parameters

< Electron beam >	
Beam energy	600 MeV
Beam current	30 mA
Bunch length	121 ps
Natural energy spread	$3.4 \cdot 10^{-4}$
Revolution frequency	5.64 MHz
<Optical klystron>	
Period length	110 mm
Number of periods	9 + 9
K value	6.18
$N_d$	45
<Ti: Sapphire laser>	
Wavelength	800 nm
Pulse energy	~2.5 mJ
Pulse duration	130 ~ 1.3 ps
Repetition rate	1 kHz

\* current address is PhLAM, Universite Lille 1, France

# takanori.tanikawa@phlam.univ-lille1.fr

## Methods

Spacial and temporal alignments between the electron beam and Ti: Sapphire laser are monitored at the light diagnostic section. The spacial alignment is performed that the electron beam and injected laser are overlapped in whole modulator part of the OK by using CCD camera. The rough temporal alignment is performed by using pin-photo diode and the precise temporal alignment is performed by using streak camera (C5680, Hamamatsu Photonics). The spectrum measurements of CHs in VUV region are performed by using VUV spectrum measurement system. The system are constructed by an aluminium coated pre-focusing mirror, a spectrometer (VMK-200-UHV, Vacuum & Optical Instruments) with a platinum coated concave replica grating of 2400 grooves/mm, and an electron multiplier tube (R5150MOD, Hamamatsu Photonics) as a detector.

## EXPERIMENTAL RESULT

As the results of spectrum measurements, VUV CHG has been observed up to 9<sup>th</sup> harmonic.

### Saturation Effect on VUV Coherent Harmonic Generation

Figure 2 and 3 show the dependences of CHs intensities on the peak power of injected laser. As shown in Figs. 2 and 3, an intensity saturation of CHs has been observed. In Fig. 2, intensities of 5<sup>th</sup>, 7<sup>th</sup>, and 9<sup>th</sup> CHs are plotted as functions of peak laser power with laser pulse duration of 870 fs. Dots represent measured values, and solid curves represent analytical simulation results [for the analytical equations, see eq. (1) ~ (4)]. As the peak laser power increases, CHs intensities also increase but tend to saturate and shows a peak around 1 GW. In Fig. 3 also, intensity saturation has been observed with laser pulse duration of 190 fs.

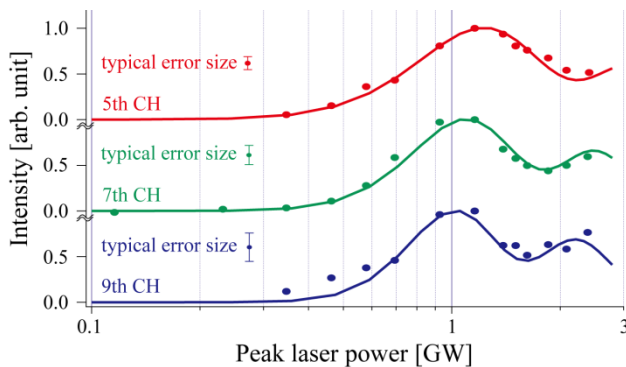


Figure 2: Measured intensities of 5th (red), 7th (green), and 9th (blue) CHs plotted as functions of the peak power of injected laser, for laser pulse duration of 870 fs. Dots represent measured values, and solid curves represent analytical simulation results.

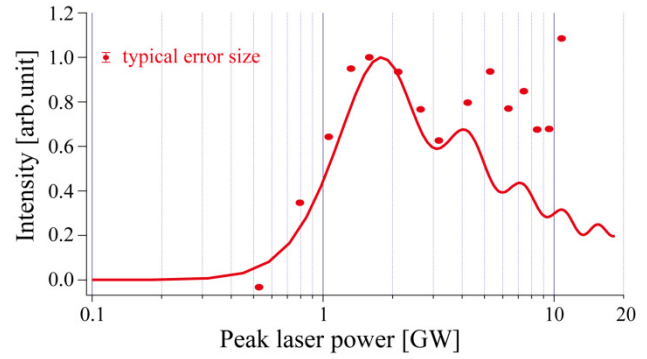


Figure 3: Measured intensity of 5th CH plotted as a function of the peak power of injected laser, for laser pulse duration of 190 fs. Dots represent measured values, and solid curve represents the analytical simulation result.

In order to compare between experimental results and analytical ones, we use the following formula which give the intensity of the  $i$ -th harmonic [11],

$$I_{\text{CH}}^{(i)} = N_e^2 F^{(i)} I_{\text{SE},1}^{(i)}, \quad (1)$$

where  $N_e$  is the number of the electrons in the bunch,  $F^{(i)}$  is the form factor given by the square of the Fourier transform of the normalized longitudinal electron density distribution, and  $I_{\text{SE},1}$  is the intensity of the SE from a single electron. Variables in the eq. (1) are given by the following formula,

$$F^{(i)} = [2J_i(i\eta)]^2, \quad (2)$$

$$\eta = 4\pi N_d \frac{\Delta E_{\text{modulation}}}{E}, \quad (3)$$

and

$$\Delta E_{\text{modulation}} = -\frac{e^2 \lambda_u B L}{4 \pi m_0 c} E_L. \quad (4)$$

Here,  $J_i$  is an  $i$ -th order Bessel function,  $\Delta E_{\text{modulation}}$  is the amplitude of energy modulation,  $E$  is the electron energy.  $e$  is the electron charge,  $\lambda_u$ ,  $B$  and  $L$  are the period length of magnet, the peak magnetic field, and the length of the OK modulator, respectively,  $m_0$  is the electron rest mass,  $c$  is the speed of light, and  $E_L$  is the amplitude of the laser electric field. In the eq. (1), the effects of the emittance and energy spread of the electron beam are ignored. About solid curves in Figs. 2 and 3, it assumes the longitudinal distribution of the laser power is Gaussian. The energy modulation was calculated as a function of the position in the electron bunch approximately. As shown in Fig. 2, our calculations reproduced the observed variation in the width and the position of the intensity peak for the three harmonics. The peak position shifts to lower peak laser powers with increasing order of the CH. Figure 3 shows that our calculation also reproduced several other peaks observed in the deep saturation

regime qualitatively. A more precise simulation, which would include three-dimensional effects, is required to achieve quantitative agreement.

To understand these results deeply, Fig. 4 shows an example of results of a one-dimensional particle tracking simulation of the bunching process in the saturated regime.

The sinusoidal energy modulation produced by the laser-electron interaction is converted to a density modulation, and the bunching is optimized at a certain peak laser power. Considering for the results of Fig. 2, the Fourier component is largest near the optimal bunching condition, where the bunching is sharpest, in the case of high-order CHs. However, for lower-order CHs, the Fourier component is largest when the electrons are slightly overbunched because of contribution of more electrons. For this reason, the lower-order CHs reach their maximum intensity at larger peak laser powers. Overbunching causes a smearing of the electron distribution but leads to further bunching subsequently at a peak laser power about 20 times greater than for the optimal condition. This regime is inaccessible to our experimental setup. However, the experiments and simulations in Fig. 3 show several peaks appearing beyond the first maximum, which can be explained by an additive interference of the double-peak structure shown in Fig. 4. When the separation of the peaks equals a multiple of the harmonic wavelength, interference produces peaks in the Fourier components, and hence in the CH intensities. The second peak in Fig. 3, which corresponds to Fig. 4, can be explained in the same manner [12].

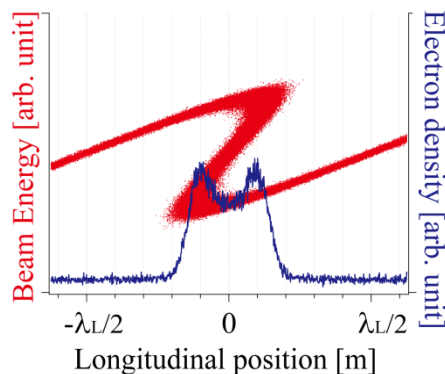


Figure 4: Simulation of the bunching process in the OK at the formation of the second peak in Fig. 3. The blue curve (longitudinal electron density distribution) effectively represents a histogram of the data in red.

## GENERATION OF SHORTER WAVELENGTH COHERENT HARMONICS

For a generation of shorter wavelength CHs at UVSOR-II and an establishment the laser seeding technology for the single-pass FEL, the seed light source by using nonlinear crystal and based on higher harmonic generation (HHG) in a gas are under development in UVSOR-II. Now the HHG system has been constructed. The target wavelength is 160 nm (5<sup>th</sup> harmonic of Ti:Sapphire laser). The HHG experiment is under studying and HHG-seeded CHG experiment will be demonstrated in the future.

## SUMMARY AND FUTURE PLAN

We have successfully observed CHs up to the 9<sup>th</sup> harmonic over a wide peak power range. In addition, we observed CH intensity oscillations after the first maximum. We compared these measurements with a one-dimensional calculation that qualitatively reproduced our experimental results, and showed that the intensity oscillation originates from the formation of the double-peak structure in the longitudinal density distribution of the electron beam. Further simulation would consider the three-dimensional distributions of the laser and the electron beams. This research is useful to the next-generation seeded FELs. Finally, HHG system for the seed light is under development for shorter wavelength CHG.

## REFERENCES

- [1] G. Lambert, et al., Nat. Phys. 4 (2008) 296.
- [2] S. Werin, et al., Nuclear Instruments and Methods in Physics Reserch A 290 (1990) 589.
- [3] R. Prazeres, et al., Nuclear Instruments and Methods in Physics Reserch A 304 (1991) 72.
- [4] C. Spezzani, et al., Nuclear Instruments and Methods in Physics Reserch A 596 (2008) 451.
- [5] L. -H. Yu, et al., Science 289 (2000) 932.
- [6] M. Hosaka, et al., UVSOR Activity Report 2007, 2008.
- [7] M. Hosaka, et al., Nuclear Instruments and Methods in Physics Research A 507 (2003) 289.
- [8] H. Zen, et al., Proceedings of FEL 09, Liverpool, England, 2009.
- [9] M. Labat, et al., Euro. Phys. Journal D, 44-1 (2007) 187.
- [10] M. Labat, et al., Phys. Rev. Lett. 101 (2008) 164803.
- [11] S. Werin, University of Lund, LUNTDX/(NTMX-1002), 1991.
- [12] T. Tanikawa, et al., Appl. Phys. Express 3 (2010) 122702.